

Analysis of MHD flow characteristics of an UCM viscoelastic flow in a permeable channel under slip conditions

M. Abbasi · M. Khaki · A. Rahbari · D. D. Ganji ·
I. Rahimipetroudi

Received: 8 October 2014 / Accepted: 10 February 2015 / Published online: 1 March 2015
© The Brazilian Society of Mechanical Sciences and Engineering 2015

Abstract In the present study, the problem of two-dimensional magneto-hydrodynamic (MHD) flow of an upper-convected Maxwell (UCM) fluid has been investigated in a permeable channel with slip at the boundaries. Employing the similarity variables, the basic partial differential equations are reduced to ordinary differential equations with Dirichlet and Neumann boundary conditions which are solved analytically and numerically using the Homotopy Analysis Method and fourth-order Runge–Kutta–Fehlberg method, respectively. The influences of the some physical parameters such as Reynolds number, slip condition, Hartman number and Deborah number on non-dimensional velocity profiles are considered. As an important outcome, comparison between HAM and numerical method shows that HAM is an exact and high-efficient method for solving these kinds of problems. Moreover, it can be found that the velocity profiles are a decreasing function of Hartmann number and Deborah number.

Keywords Homotopy analysis method · Slip condition · Magneto-hydrodynamic · Permeable channel · Upper-convected Maxwell fluid

List of symbols

Re_w	Reynolds number
M	Hartman number
k	Slip parameter
De	Deborah number
HAM	Homotopy analysis method
NUM	Numerical method
\hbar	Auxiliary parameter
\mathcal{H}	Auxiliary function
\mathcal{L}	Linear operator of HAM
\mathcal{N}	Non-linear operator
v^*	Velocity component in y -direction
u^*	Velocity component in x -direction
x	Dimensionless horizontal coordinate
y	Dimensionless vertical coordinate
x^*	Distance in x -direction parallel to the plates
y^*	Distance in y -direction parallel to the plates

Technical Editor: Monica Feijo Naccache.

M. Abbasi · M. Khaki · D. D. Ganji (✉)
Department of Mechanical Engineering, Sari Branch, Islamic Azad University, Sari, Iran
e-mail: ddg_davood@yahoo.com;
iman.rahimipetroudi@gmail.com

A. Rahbari
Department of Mechanical Engineering, Shahid Rajaei Teacher Training University (SRRTU), Tehran, Iran

I. Rahimipetroudi
Young researchers Club, Sari Branch, Islamic Azad University, Sari, Iran

Greek symbols

ρ	Density of the fluid
λ	Relaxation time
ν	Kinematic viscosity
β	Of sliding friction

1 Introduction

The flow problem in porous tubes or channels received much attention in recent years because of its various applications in biomedical engineering, for example in the dialysis of blood in artificial kidney, in the flow of blood in the

capillaries, in the flow in blood oxygenators, as well as in many other engineering areas such as the design of filters, in transpiration cooling boundary layer control and gaseous diffusion. Because of its relevance to a wide variety of situations, convection in porous media is a well-developed field of investigation. Over recent decades, it has generally been recognized that some rheological complex fluids such as polymer solutions, blood, paints, butter, synovial fluid, saliva, soups, jams, ice-creams and certain oils cannot be adequately described by the Navier–Stokes theory. Because of this, several constitutive equations and flows for non-Newtonian fluids have been developed [1]. Undoubtedly, the equations of motion of these fluids are highly nonlinear and with higher order than the Navier–Stokes equations. One important and simple model that has been used to describe the rheological characteristics exhibited by certain fluids is the second-grade fluid. However, the second-grade fluid model [2] does not give reasonable results for flows of highly elastic fluids (polymer melts) that occur at high Deborah number [3]. For such situations the upper-convected Maxwell (UCM) model is quite appropriate. The suction flow in a channel for a UCM fluid was examined by Choi et al. [4]. More recently, Sadeghy et al. [5] examined the hydrodynamic flow of the UCM model over a steadily moving plate. Recently, the subject of hydromagnetics has attracted the attention of many authors, due not only to its inherent interest, but also to its many applications to problems of geophysical and astrophysical significance. The solution of the problem of magneto-hydrodynamic (MHD) flow of a Newtonian fluid through a flat channel is known and is usually given in textbooks on fluid dynamics. For large values of the Hartman number, the flow exhibits the characters of boundary layer, namely the Hartman layers. These also manifest themselves in ducts with other shapes. A particularly large literature exists on the solution of MHD flows through rectangular ducts [6–13]. These scientific problems and phenomena are modeled by

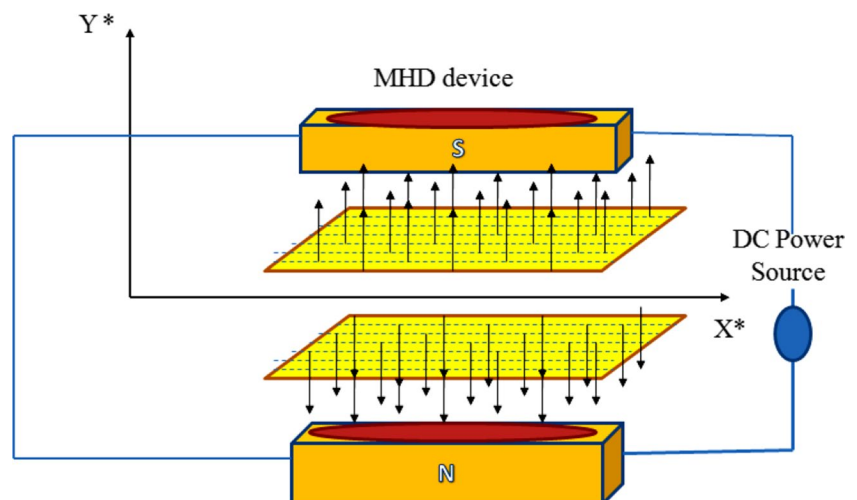
ordinary or partial differential equations. In most cases, these problems do not admit analytical solution, so these equations should be solved using special techniques. In recent years, much attention has been devoted to the newly developed methods to construct an analytic solution of equation; such methods include the Adomian decomposition method [14] and Perturbation techniques. Perturbation techniques are too strongly dependent upon the so-called “small parameters” [15]. Thus, it is worthwhile to develop some new analytic techniques independent of small parameters. One of these techniques is Homotopy Analysis Method (HAM), which was introduced by Liao [16–21]. This method has been successfully applied to solve many types of nonlinear problems [22–26].

In this Letter, the equations of the two-dimensional MHD of an upper-convected Maxwell fluid in a permeable channel with slip at the boundaries are solved through HAM. The effects of Reynolds number Re_w , slip condition k , Hartman number M and Deborah number De on velocity distributions are examined in detail. The convergence of the series solution is also explicitly discussed. The auxiliary parameter validity is different for each Reynolds number Re_w , slip condition k , Hartman number M and Deborah number De . The afore-mentioned method gives rapidly convergent series with specific significant features for each scheme. Most authors studied permeable channel at various situations with no-slip boundary condition. The main objective of the present paper is to study a steady incompressible laminar UCM fluid flow through a porous channel with slip condition on walls.

2 Problem statement and mathematical formulation

Let us consider the steady laminar flow of an incompressible and electrically conducting fluid in a channel with slip

Fig. 1 Schematic diagram of the permeable channel



at the permeable walls as shown in Fig. 1. The slip boundary conditions are exerted on walls. The uniform magnetic field B_0 is imposed along the y -axis. It is assumed that the magnetic Reynolds Number is small and the induced magnetic field due to the motion of the electrically conducting fluid is negligible. It is also assumed that the electrical conductivity of fluid σ is constant and the external electric field is zero.

The constitutive equation for a Maxwell fluid is [27].

$$T = -pI + S, \tag{1}$$

where T is the Cauchy stress tensor and the extra-stress tensor S satisfies.

$$S + \lambda \left(\frac{dS}{dt} - LS - SL^T \right) = \mu A_1 \tag{2}$$

In which μ is the viscosity, λ is the relaxation time and the Rivlin-Ericksen tensor A_1 is defined through

$$A_1 = \nabla V + (\nabla V)^T \tag{3}$$

For the steady two-dimensional flow, the equations of continuity and momentum for the magneto-hydrodynamic flow are [28, 29].

$$\frac{\partial u}{\partial x} + \frac{\partial v}{\partial y} = 0, \tag{4}$$

$$\rho \left(u \frac{\partial u}{\partial x} + v \frac{\partial u}{\partial y} \right) = -\frac{\partial p}{\partial x} + \frac{\partial S_{xx}}{\partial x} + \frac{\partial S_{xy}}{\partial y} - \sigma B_0^2 u, \tag{5}$$

$$\rho \left(u \frac{\partial v}{\partial x} + v \frac{\partial v}{\partial y} \right) = -\frac{\partial p}{\partial x} + \frac{\partial S_{yx}}{\partial x} + \frac{\partial S_{yy}}{\partial y}, \tag{6}$$

where ρ is the fluid density and S_{xx} , S_{xy} , S_{yx} and S_{yy} are the components of the extra-stress tensor. After some modification, the governing continuity and momentum equations for the motion can be written as follows [30, 31]

$$\frac{\partial u^*}{\partial x^*} + \frac{\partial v^*}{\partial y^*} = 0 \tag{7}$$

$$u^* \frac{\partial u^*}{\partial x^*} + v^* \frac{\partial u^*}{\partial y^*} + \lambda \left[u^{*2} \frac{\partial^2 u^*}{\partial x^{*2}} + v^{*2} \frac{\partial^2 u^*}{\partial y^{*2}} + 2u^* v^* \frac{\partial^2 u^*}{\partial x^* \partial y^*} \right] = v \frac{\partial^2 u^*}{\partial y^{*2}} - \frac{\sigma B_0^2}{\rho} u^*, \tag{8}$$

where (u^*, v^*) are the fluid velocity components along x^* - and y^* -directions, respectively. The flow is symmetric about the center line of the channel, $y^* = 0$ and we only focus our attention on the flow in the region $0 < y^* < H$. The boundary conditions for this problem can be written as follows [32]:

$$y^* = 0: \frac{\partial u^*}{\partial y^*} = 0, \quad v^* = 0, \tag{9}$$

Table 1 The results of h -validity for different value of De , k , M and Re_w

M	$De = 0.1$		$De = 0.9$		$Re_w = +10$		$Re_w = -10$	
	$k = 0.1$	$k = 0.9$	$k = 0.1$	$k = 0.9$	$k = 0.1$	$k = 0.9$	$k = 0.1$	$k = 0.9$
1	$-2.0 < h < 0.2$	$-1.4 < h < 0.4$	$-1.5 < h < -0.1$	$-1.8 < h < 0.0$	$-1.8 < h < -0.1$	$-1.8 < h < 0.0$	$-1.8 < h < -0.5$	$-1.9 < h < 0.0$
2	$-1.4 < h < 0.3$	$-1.1 < h < 0.0$	$-1.7 < h < -0.1$	$-1.4 < h < 0.1$	$-1.7 < h < -0.1$	$-1.4 < h < 0.1$	$-2.2 < h < -0.5$	$-2.0 < h < 0.0$
3	$-1.1 < h < 0.5$	$-0.8 < h < 0.0$	$-1.0 < h < 0.0$	$-1.0 < h < 0.0$	$-1.0 < h < 0.0$	$-1.0 < h < 0.0$	$-0.7 < h < 0.0$	$-0.8 < h < -0.2$
4	$-0.8 < h < 0.0$	$-0.6 < h < 0.0$	$-0.7 < h < -0.1$	$-0.7 < h < 0.0$	$-0.7 < h < -0.1$	$-0.7 < h < 0.0$	$-0.9 < h < 0.0$	$-1.5 < h < 0.0$
5	$-0.6 < h < 0.0$	$-0.5 < h < 0.0$	$-0.6 < h < 0.0$	$-0.5 < h < 0.0$	$-0.6 < h < 0.0$	$-0.5 < h < 0.0$	$-1.0 < h < 0.0$	$-1.4 < h < 0.1$

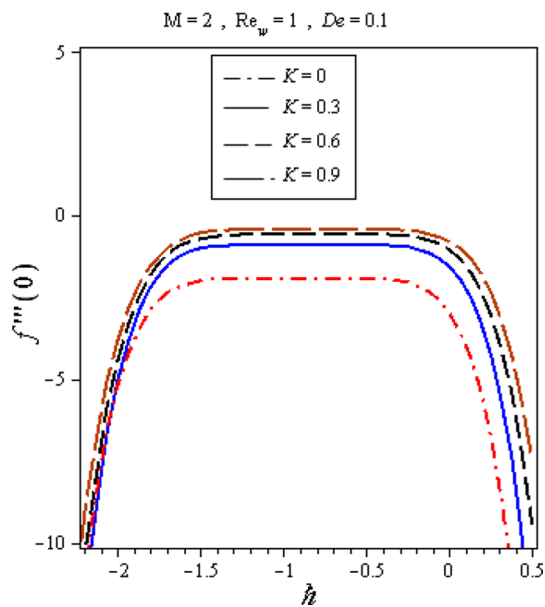


Fig. 2 The h -validity for $M = 2$, $De = 0.1$, $Re_w = 1$ and different value of k

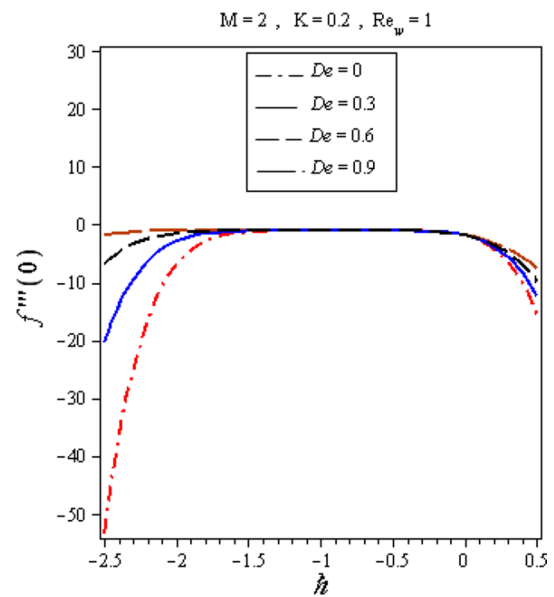


Fig. 3 The h -validity for $M = 2$, $K = 0.2$, $Re_w = 1$ and different value of De

$$y^* = H: -\beta u^* = \frac{\partial u^*}{\partial y^*}, \quad v^* = V_w, \tag{10}$$

where β and V_w are the coefficients of sliding friction and characteristic wall suction velocity, respectively. The following dimensionless variables are introduced.

$$\begin{aligned} x &= \frac{x^*}{H}; & y &= \frac{y^*}{H}; & u^* &= -V_w x f'(y); \\ v^* &= V_w f(y); & k &= \frac{\mu}{H\beta}. \end{aligned} \tag{11}$$

Equation (1) is automatically satisfied. And Eqs. (2)–(4) may be written as:

$$f''' - M^2 f' + Re_w (f'^2 - f f'') + De (2f f' f'' - f^2 f''') = 0 \tag{12}$$

The boundary conditions become

$$\begin{aligned} y = 0: & \quad f'' = 0; \quad f = 0. \\ y = 1: & \quad f' = -k f''; \quad f = 1. \end{aligned} \tag{13}$$

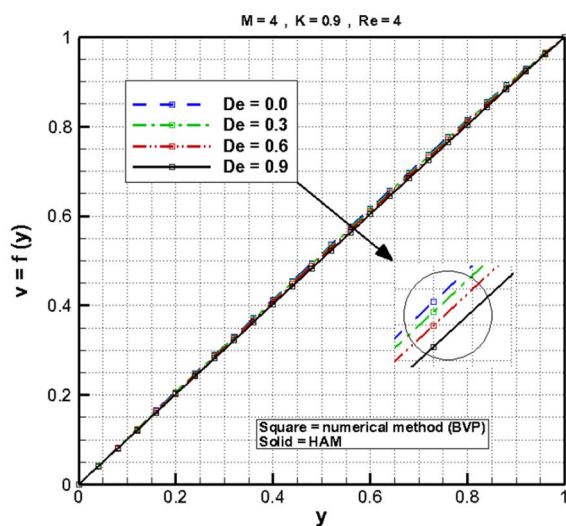
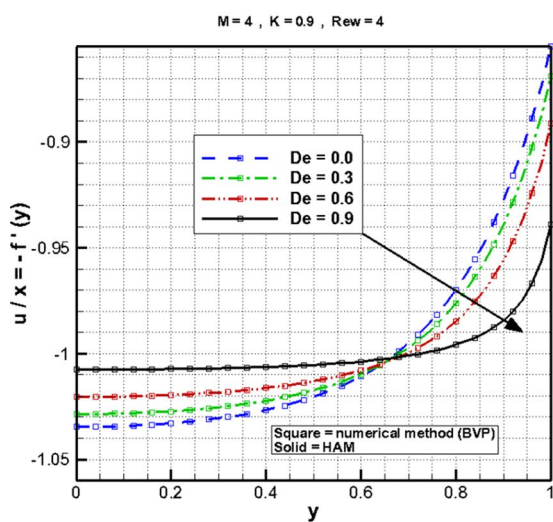


Fig. 4 The comparison between the numerical, HAM solution for $f(y)$ and $f'(y)$ when $Re_w = 4$, $K = 0.9$, $M = 4$, $h = -0.8$ and different values of De

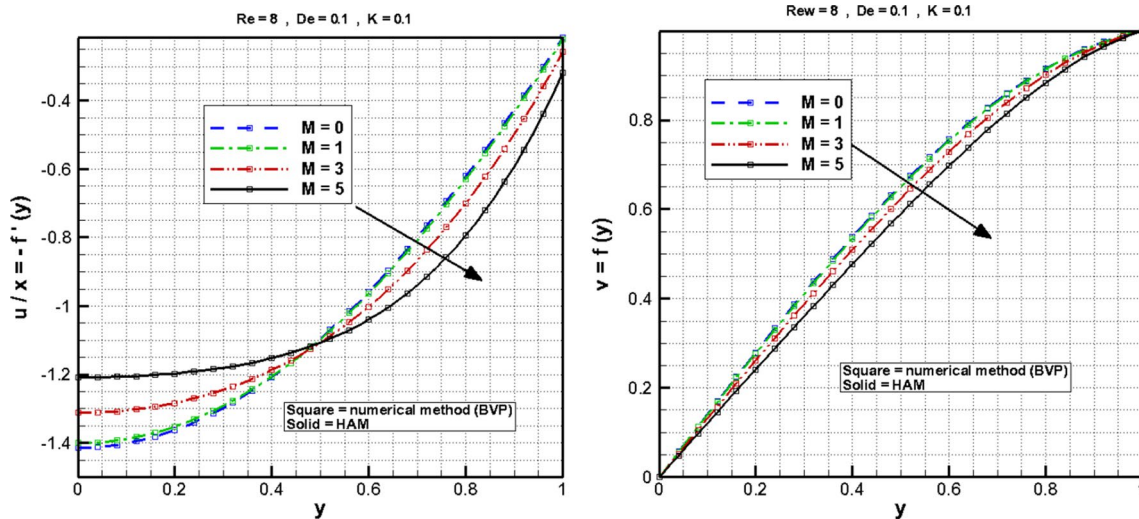


Fig. 5 The comparison between the numerical, HAM solution for $f(y)$ and $f'(y)$ when $Re_w = 8, K = 0.1, De = 0.1, \hat{h} = -0.8$ and different values of M

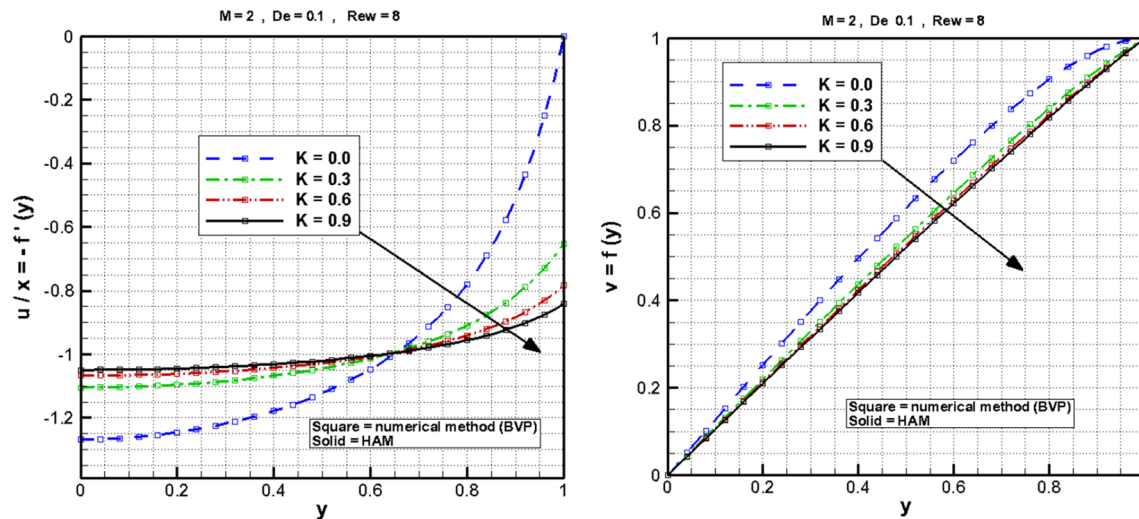


Fig. 6 The comparison between the numerical, HAM solution for $f(y)$ and $f'(y)$ when $Re_w = 8, De = 0.1, M = 2, \hat{h} = -0.8$ and different values of K

Against the differential equation of the model which is in third order, there are four boundary conditions for this problem. Some authors satisfy boundary conditions in the initial guess function. In the present study, creatively with derivation of Eq. (12) and introduce fourth-order differential equation we can satisfy all of boundary conditions in main equation. Then we have,

$$f''' - M^2 f'' + Re_w (f' f'' - f f''') + De (2f'^2 f'' - 2f f'''^2 + f^2 f'''') = 0 \tag{14}$$

Here, $Re_w = \frac{V_w H}{\nu}$ is the Reynolds number, $De = \frac{\lambda V_w^2}{\nu}$ is the Deborah number, and $M^2 = \frac{\sigma B_0^2 H}{\mu}$ is the Hartman

number, where $Re_w > 0$ corresponds to suction and $Re_w < 0$ is for injection.

3 Application of homotopy analysis method

For HAM solutions, we choose the initial guess and auxiliary linear operator in the following form:

$$f_0(y) = -\frac{1}{2(3k+1)} y^3 + \frac{3(2k+1)}{2(3k+1)} y, \tag{15}$$

$$L(f) = f'''' , \tag{16}$$

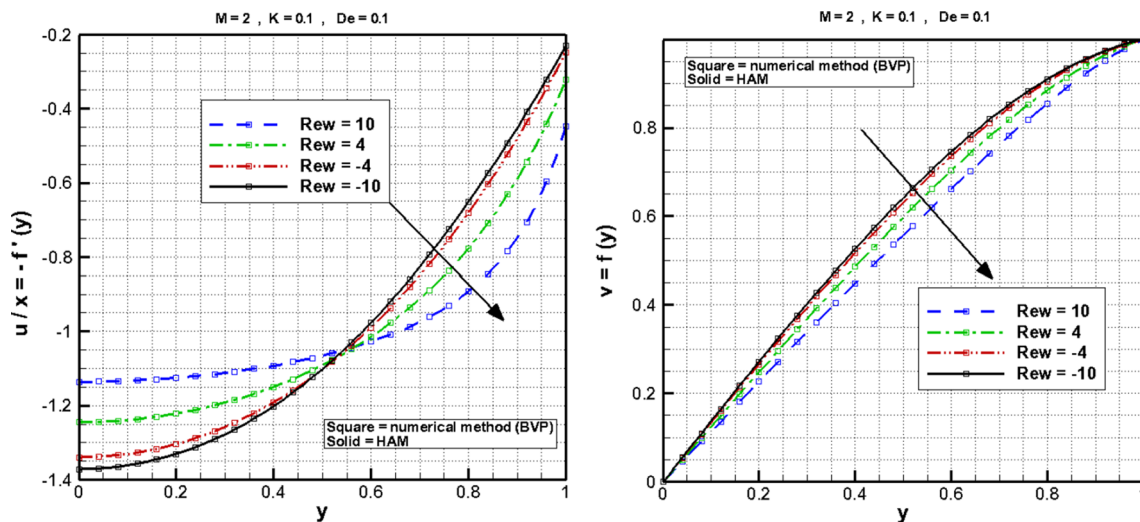


Fig. 7 The comparison between the numerical, HAM solution for $f(y)$ and $f'(y)$ when $De = 0.1, K = 0.1, M = 2, \hbar = -0.8$ and different values of Re_w

Table 2 The results of HAM and numerical methods for $f(y)$ and $f'(y)$ for $De = 0.1, k = 0.1, M = 0$ and $Re_w = 4$

y	$f(y)$			$f'(y)$		
	HAM	NUM	Error	HAM	NUM	Error
0.00	0.0000000000	0.0000000000	0.0000000000	1.40413030	1.40412452	0.00000578
0.05	0.0701545723	0.070154283	0.000000289	1.40101384	1.40100814	0.00000570
0.10	0.139997550	0.139996981	0.000000569	1.39166755	1.39166207	0.00000548
0.15	0.209217650	0.209216817	0.000000833	1.37610088	1.37609577	0.00000511
0.20	0.209217650	0.209216817	0.000001080	1.35433002	1.37609577	0.00000459
0.25	0.344547639	0.344546348	0.000001290	1.32637866	1.32637470	0.00000396
0.30	0.410039617	0.410038147	0.000001470	1.29227887	1.29227567	0.00000320
0.35	0.473673743	0.473672132	0.000001610	1.25207237	1.25207001	0.00000236
0.40	0.535145948	0.473672132	0.000001710	1.20581184	1.20581039	0.00000145
0.45	0.594155105	0.594153351	0.000001750	1.20581184	1.15356206	0.00000049
0.50	0.650403705	0.650401951	0.000001750	1.09540402	1.09540452	0.00000050
0.55	0.703598603	0.650401951	0.000001700	1.09540402	1.03143337	0.00000150
0.60	0.753451885	0.753450277	0.000001610	0.961759843	0.961762230	0.00000240
0.65	0.799681804	0.799680337	0.000001470	0.886521503	0.886524729	0.00000320
0.70	0.842013847	0.842012558	0.000001290	0.805872580	0.805876515	0.00000390
0.75	0.880181868	0.880180791	0.000001080	0.719992837	0.719997311	0.00000450
0.80	0.913929366	0.913928521	0.000000845	0.629088180	0.629092973	0.00000480
0.85	0.913929366	0.943010220	0.000000605	0.533392682	0.533397521	0.00000480
0.90	0.967193183	0.967192807	0.000000376	0.433170588	0.433175149	0.00000460
0.95	0.986257359	0.986257206	0.000000153	0.328718280	0.328722174	0.00000390
1.00	1.000000000	1.000000000	0.000000000	0.220366140	0.220368909	0.00000280

$$L \left(\frac{1}{6}c_1 y^3 + \frac{1}{2}c_2 y^2 + c_3 y + c_4 \right) = 0, \tag{17}$$

where c_i ($i = 1, 2, 3, 4$) are constants. Let $P \in [0, 1]$ denotes the embedding parameter and \hbar indicates non-zero auxiliary parameters. We then construct the following equations:

3.1 Zeroth-order deformation equations

$$(1 - P)L[F(y; p) - f_0(y)] = p\hbar H(y)N[F(y; p)] \tag{18}$$

$$F(0; p) = 0; \quad F''(0; p) = 0, \quad F(1; p) = 1, \tag{19}$$

$$kF''(1; p) + F'(1; p) = 0$$

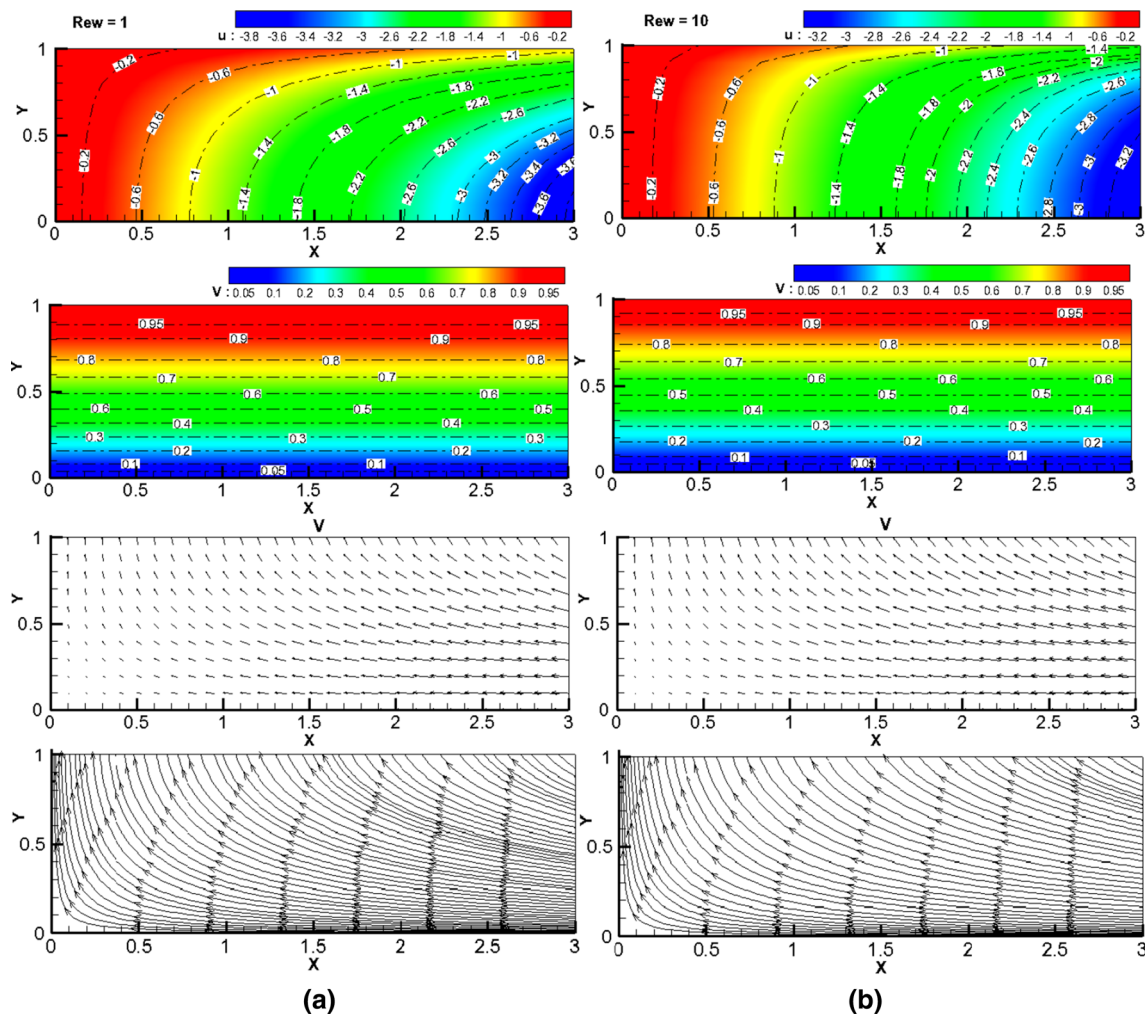


Fig. 8 Effects of Re_w on the velocity components u^* and v^* contours and vector V , when **a** $Re_w = 1$ and **b** $Re_w = 10$ at $(k = 0.1, M = 2, De = 0.1, \hbar = -0.8)$

$$\begin{aligned}
 N[F(y; p)] = & \frac{d^4 F(y; p)}{dy^4} + \text{Re} \left[\frac{dF(y; p)}{dy} \frac{d^2 F(y; p)}{dy^2} - F(y; p) \frac{d^3 F(y; p)}{dy^3} \right] - M^2 \frac{d^2 F(y; p)}{dy^2} \\
 & + \text{De} \left[2 \left(\frac{dF(y; p)}{dy} \right)^2 \frac{d^2 F(y; p)}{dy^2} - 2F(y; p) \left(\frac{d^2 F(y; p)}{dy^2} \right)^2 + (F(y; p))^2 \frac{d^4 F(y; p)}{dy^4} \right].
 \end{aligned} \tag{20}$$

For $p = 0$ and $p = 1$ we have

$$F(y; 0) = f_0(y) \quad F(y; 1) = f(y) \tag{21}$$

When p increases from 0 to 1 then $F(y; p)$ varies from $f_0(y)$ to $f(y)$. By Taylor’s theorem and using Eq. (20), $F(y; p)$ can be expanded in a power series of p as follows:

$$F(y; p) = f_0(y) + \sum_{m=1}^{\infty} f_m(y) p^m, \quad f_m(y) = \left. \frac{1}{m!} \frac{\partial^m (F(y; p))}{\partial p^m} \right|_{p=0} \tag{22}$$

In which \hbar is chosen in such a way that this series is convergent at $p = 1$; therefore, we have through Eq. (21) that

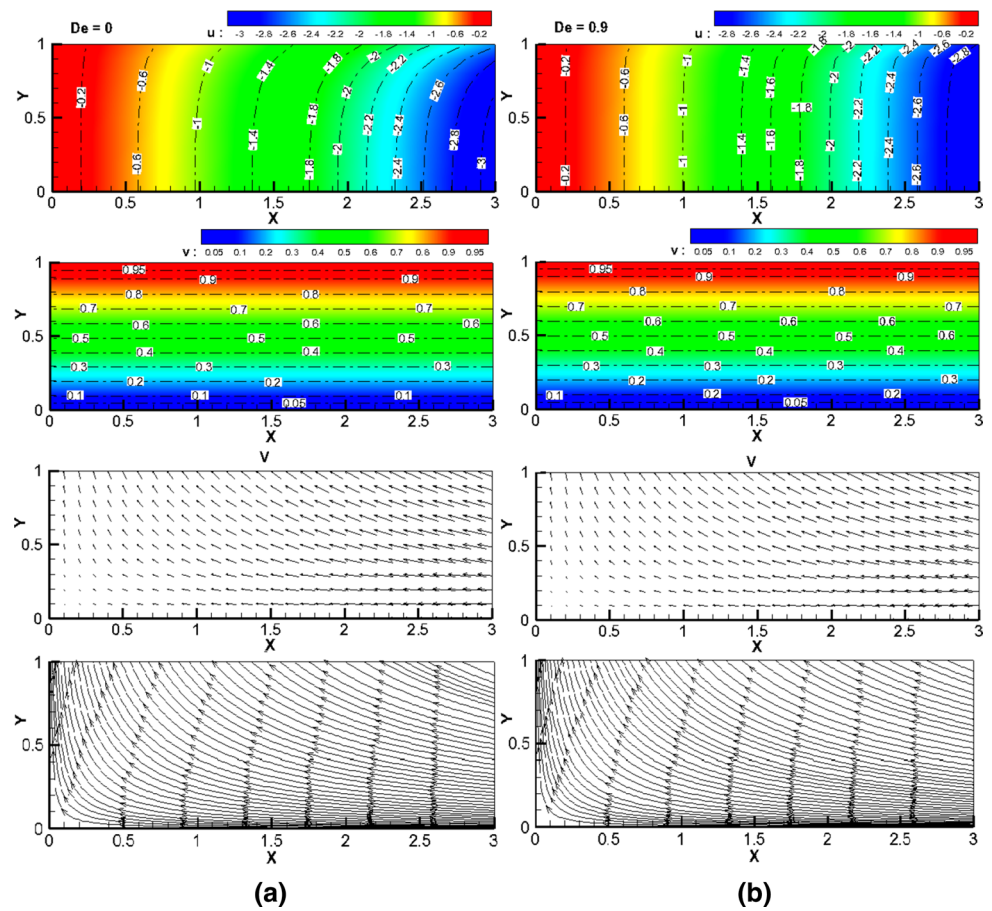
$$f(y) = f_0(y) + \sum_{m=1}^{\infty} f_m(y), \tag{23}$$

3.2 mth-order deformation equations

$$L[f_m(y) - \chi_m f_{m-1}(y)] = \hbar H(y) R_m(y) \tag{24}$$

$$\begin{aligned}
 F_m(0; p) = 0; \quad F_m''(0; p) = 0, \quad F_m(1; p) = 0, \\
 kF_m''(1; p) + F_m'(1; p) = 0
 \end{aligned} \tag{25}$$

Fig. 9 Effects of De on the velocity components u^* and v^* contours and vector V , when **a** $De = 0.0$ and **b** $De = 0.9$ at $k = 0.9$, $M = 4$, $Re_w = 4$, $\hbar = -0.8$



$$R_m(y) = f_{m-1}''' + \sum_{k=0}^{m-1} \left[\text{Re}(f'_{m-1-k} f''_k - f_{m-1-k} f_k''') + De f'_{m-1-k} \left(\sum_{l=0}^k (2f'_{k-l} f_l'') \right) - Def_{m-1-k} \left(\sum_{l=0}^k (2f''_{k-l} f_l' - f_{k-l} f_l''''') \right) \right] - M^2 f_{m-1}'' \tag{26}$$

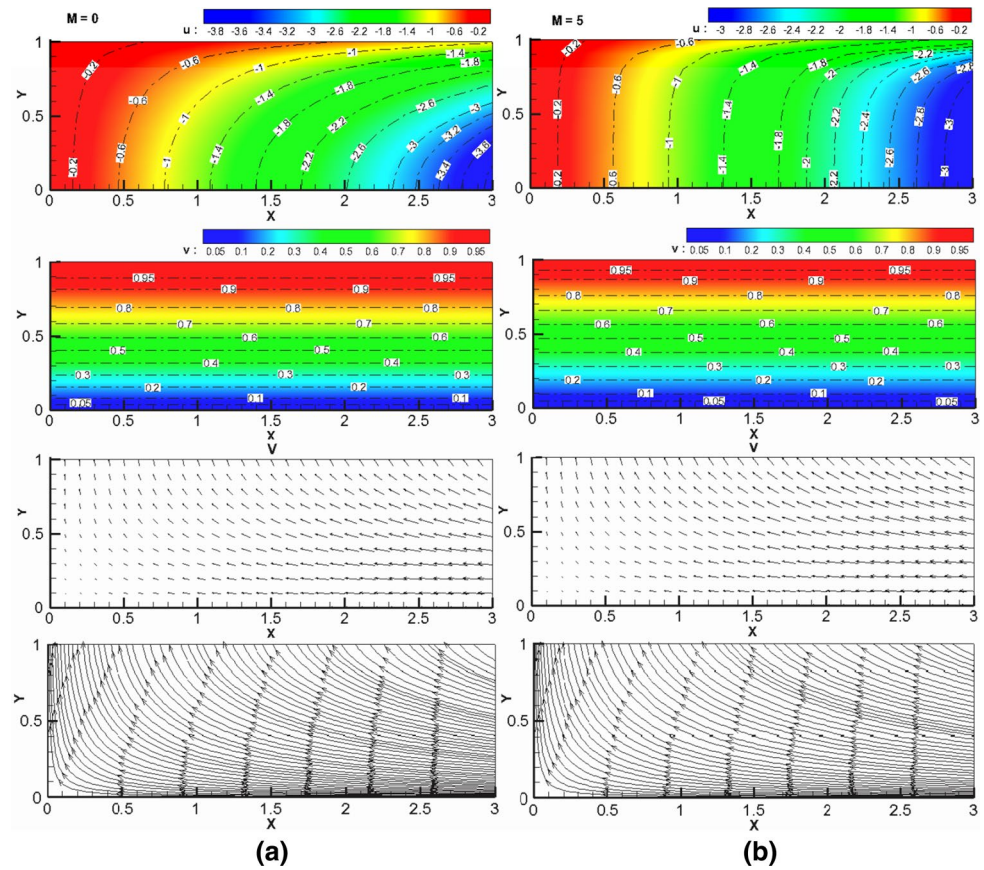
Now we determine the convergency of the result, the differential equation and the auxiliary function according to the solution expression. So let us assume:

$$H(y) = 1 \tag{27}$$

We have found the answer by maple analytic solution device. The first deformation of the solution is presented below

$$f_1(y) = -\frac{5\hbar}{672} \frac{De y^9}{(3k+1)^3} - \frac{3\hbar}{2} \frac{(-0.0071429Re_w k - 0.042857De - 0.0023810Re_w - 0.085714De k)y^7}{27k^3 + 27k^2 + 9k + 1} - \frac{3\hbar}{2} \frac{(-0.15000M^2 k^2 - 0.10000M^2 k - 0.016667M^2 + 0.30000De k^2 + 0.30000De k + 0.075000De)y^5}{27k^3 + 27k^2 + 9k + 1} + \frac{\hbar}{840} \left[\frac{(3780De k^3 - 1890M^2 k^3 - 189Re_w k^2 + 2268De k^2 - 1638M^2 k^2 - 90Re_w k - 462M^2 k + 468De k)y^3}{1 + 54k^2 + 12k + 108k^3 + 81k^4} + \frac{(-9Re_w + 52De - 42M^2)y^3}{1 + 54k^2 + 12k + 108k^3 + 81k^4} \right] - \frac{\hbar}{1120} \left[\frac{(-8Re_w - 96Re_w k - 1764M^2 k^3 1440De k^2 + 77De k - 364M^2 k)y}{1 + 54k^2 + 12k + 108k^3 + 81k^4} + \frac{(-1428M^2 k^2 + 3528De k^3 - 216Re_w k^2 - 28M^2 + 7De)y}{1 + 54k^2 + 12k + 108k^3 + 81k^4} \right] \tag{28}$$

Fig. 10 Effects of M on the velocity components u^* and v^* contours and vector V , when **a** $M = 0$ and **b** $M = 5$ at $k = 0.1$, $De = 0.1$, $Re_w = 8$, $\hbar = -0.8$



The solutions $f(y)$ were too long to be mentioned here; therefore, they are shown graphically

4 Convergence of the HAM solution

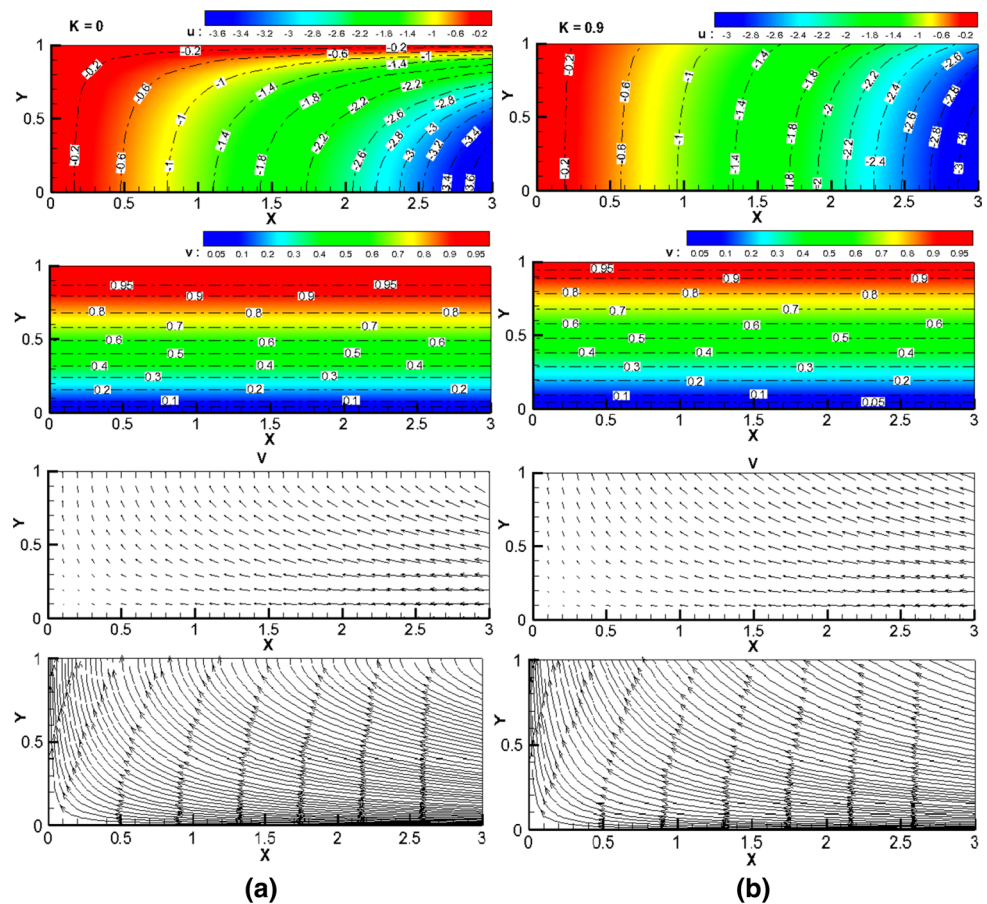
As pointed out by Liao [12], the convergence and rate of approximation for the HAM solution strongly depend on the value of auxiliary parameter \hbar . The appropriate region for \hbar is a horizontal line segment, which indicates a numerical range for having a convergent series solution. As mentioned we can adjust \hbar to get most accurate solution, but in this problem we have a wide acceptable range values of \hbar ; therefore, we can take \hbar from this region, as you can see in Table 1. In the following, to investigate the range of admissible values of the auxiliary parameter \hbar , take the case of $f'''(0)$ at $M = 2$, $De = 0.1$, $Re_w = 1$ and different value of slip number as shown in Fig. 2. As can be seen, the range of admissible values of the auxiliary parameter \hbar equals $-1.5 < \hbar < 0.0$. In the same manner, the admissible values of \hbar at $k = 0.2$, $Re_w = 1$, $M = 2$ and different values of Deborah number are shown in Fig. 3.

5 Results and discussion

In the present study, HAM method is applied to obtain an explicit analytic solution of an upper-convected maxwell fluid in a permeable channel with slip at the boundaries in the presence of uniform magnetic field (Fig. 1). HAM is used for this aim due to many advantages which some of them are described by Liao [12, 34] as follows,

- a. Unlike all other analytic techniques, HAM provides us with great freedom to express solutions of a given nonlinear problem by means of different base functions.
- b. HAM always provides us with a family of solution expressions in the auxiliary parameter \hbar , even if a nonlinear problem has a unique solution, so the auxiliary parameter \hbar provides us with an additional way to conveniently adjust and control the convergence region and rate of solution series.
- c. Unlike perturbation techniques, the Homotopy Analysis Method is independent of any small or large quantities. So, the Homotopy Analysis Method can be applied no matter if governing equations and boundary/initial

Fig. 11 Effects of k on the velocity components u^* and v^* contours and vector V , when **a** $k = 0.0$ and **b** $k = 0.9$ at $De = 0.1$, $M = 2$, $Re_w = 8$, $h = -0.8$



conditions of a given nonlinear problem contain small or large quantities or not.

First, the present code is validated by comparing the obtained results with the numerical method for different values of active parameters, shown in Figs. 4, 5, 6, 7 and Table 2. The numerical solution is performed using the algebra package Maple 16.0, to solve the present problem. The package uses a second-order difference scheme combined with an order bootstrap technique with mesh-refinement strategies: the difference scheme is based on either the trapezoid or midpoint rules; the order improvement/accuracy enhancement is either Richardson extrapolation or a method of deferred corrections. The midpoint method, also known as the fourth-order Runge–Kutta–Fehlberg method, improves the Euler method by adding a midpoint in the step which increases the accuracy by one order. Thus, the midpoint method is used as a suitable numerical technique [35, 36]. By observing the overall pattern, it is noticed that this comparison shows an excellent agreement, so that we are confident that the present results are accurate.

This investigation is completed by depicting the effects of some important parameters Reynolds number Re_w , Deborah number De , Hartman number M and slip condition k

to determine how these parameters affect the velocity components. Effect of Reynolds number (Re_w) on velocities contours at $k = 0.1$, $M = 2$, $De = 0.1$ is shown in Fig. 8. As can be seen, increasing the Re number makes a decrease in velocity profiles also it is worth to mention that the Reynolds number indicates the relative significance of the inertia effect compared to the viscous effect.

On the other hand, Fig. 9 shows the effect of viscoelastic material parameter, i.e. Deborah number on the velocity components when $M = 4$, $Re_w = 4$, $k = 0.9$. The Deborah number (De) represents the ratio of a relaxation time, and the characteristic time scale of an experiment or a computer simulation probing the response of the material [31, 33]. As can be seen, an increase in the elastic parameter is noticed to decrease both u - and v -velocity components at any given point. It means that the smaller the Deborah number, the more fluid the material appears. Higher De values imply a strongly elastic behavior. Figure 10 shows the effect of Hartman number M on the velocity components for $k = 0.1$, $De = 0.1$, $Re_w = 8$. Increase in the magnetic parameter leads to decrease in the velocity components and contours at given point. This is due to the fact that applied transverse magnetic field produces a damping in the form of Lorentz force thereby decreasing the magnitude of

velocity. The drop in velocity as a consequence of increase in the strength of magnetic field is observed.

Finally, Fig. 11 shows the effect of slip condition on the velocity contours when $De = 0.1$, $M = 2$, $Re_w = 8$. As seen in these figures, by decreasing slip condition, the slip coefficient β increases and the flow over the border desires to no-slip condition.

6 Conclusion

In the present paper, the problem of a MHD flow of an upper-convected Maxwell viscoelastic fluid in a permeable channel with slip at the boundaries has been studied for the analytical solution using homotopy analysis method (HAM). The effects of physical flow parameters such as the Reynolds number, Deborah number, Hartman number and slip condition on the flow characteristics have been examined. As a main outcome from the present study:

- It is observed that the results of HAM are in excellent agreement with numerical ones, so HAM can be used for finding analytical solutions of equations in science and engineering problems simplicity. Also, in HAM, we can choose \hbar in such a way that we get most accurate solution and this is the most important feature of this technique.
- The results show that increase in the M Hartman number associates with the reduction in velocity profile. Moreover, it is worth to mention that the velocity patterns are minimally influenced by the changes in De Deborah number parameter.
- In addition, the flow over the border desires to no-slip condition by increasing in the values of slip parameter k .

References

1. Fetecau C, Fetecau C (2003) A new exact solution for the flow of a Maxwell fluid past an infinite plate. *Int J Non-Lin Mech* 38:423–427
2. Sadeghy K, Sharifi M (2004) Local similarity solution for the flow of a “second-grade” viscoelastic fluid above a moving plate. *Int J Non-Lin Mech* 39:1265–1273
3. Bird RB, Armstrong RC, Hassager O (1987) Dynamics of polymeric liquids. vols I and II. Wiley, New York
4. Choi JJ, Rusak Z, Tichy JA (1999) Maxwell fluid suction flow in a channel. *J Non-Newton Fluid Mech* 85:165–187
5. Sadeghy K, Najafi AH, Saffaripour M (2005) Sakiadis flow of an upper-convected Maxwell fluid. *Int J Non-Lin Mech* 40:1220–1228
6. Hunt JCR (1965) Magnetohydrodynamic flow in rectangular ducts. *J Fluid Mech* 21:577–590
7. Ziabakhsh Z, Domairry G (2008) Solution of laminar viscous flow in semi porous channel in the presence of a uniform magnetic field by using homotopy analysis method, accepted in communications in nonlinear science and numerical simulation
8. Ganji DD, Hashemi Kachapi Seyed H (2011) Analytical and numerical method in engineering and applied science. *Progress Nonlinear Sci* 3:1–579
9. Sheikholeslami M, Hatami M, Ganji DD (2014) Nano fluid flow and heat transfer in a rotating system in the presence of a magnetic field. *J Mol Liq* 190:112–120
10. Sheikholeslami M, Hatami M, Ganji DD (2013) Analytical investigation of MHD nanofluid flow in a semi-porous channel. *Powder Technol* 246:327–336
11. Sheikholeslami M, Ganji DD (2015) Entropy generation of nanofluid in presence of magnetic field using lattice boltzmann method. *Physica A* 417:273–286
12. Sheikholeslami M, Gorji-Bandpy M, Ganji DD (2014) Lattice Boltzmann method for MHD natural convection heat transfer using nanofluid. *Powder Technol* 254:82–93
13. Sheikholeslami M, Gorji-Bandpy M, Ganji DD (2013) Numerical investigation of MHD effects on Al₂O₃–water nanofluid flow and heat transfer in a semi-annulus enclosure using LBM. *Energy* 60:501–510
14. Adomian G (1992) A review of the decomposition method and some recent results for nonlinear equation. *Math Comput Model* 13(7):17
15. Nayfeh AH (2000) Perturbation methods. Wiley, New York
16. Liao SJ (1992) The proposed homotopy analysis technique for the solution of nonlinear problems. Ph.D. thesis, Shanghai Jiao Tong University
17. Liao SJ (1995) An approximate solution technique not depending on small parameters: a special example. *Int J Non-Linear Mech* 30:371–380
18. Rashidi MM, Parsa AB, B’eg OA, Shamekhi L, Sadri SM, B’eg TA (2014) Parametric analysis of entropy generation in magneto-hemodynamic flow in a semi-porous channel with OHAM and DTM. *Appl Bion Biomech* 11:47–60
19. Liao SJ (2003) Beyond perturbation: introduction to the homotopy analysis method. Chapman & Hall, CRC Press, Boca Raton
20. Liao SJ, Cheung KF (2003) Homotopy analysis of nonlinear progressive waves in deep water. *J Eng Math* 45(2):103–116
21. Liao SJ (2004) On the homotopy analysis method for nonlinear problems. *Appl Math Comput* 47(2):499–513
22. Rashidi MM, Domairry G, Dinarvand S (2009) Approximate solutions for the Burger and regularized long wave equations by means of the homotopy analysis method. *Commun Nonlinear Sci Numer Simulat* 14(3):708–717
23. Domairry G, Fazeli M (2009) Homotopy Analysis method to determine the fin efficiency of convective straight fins with temperature dependent thermal conductivity. *Commun Nonlinear Sci Numer Simulat* 14(2):489–499
24. Ganji DD, Kachapi SH (2011) Analysis of nonlinear equations in fluids. *Prog Nonlinear Sci* 3:1–294
25. Xu H, Liao SJ (2008) Dual solutions of boundary layer flow over an upstream moving plate. *Commun Nonlinear Sci Numer Simulat* 13(2):350–358
26. Domairry G, Nadim N (2008) Assessment of homotopy analysis method and homotopy perturbation method in non-linear heat transfer equation. *Int Commun Heat Mass Transf* 35(1):93
27. Raftari B, Yildirim A (2010) The application of homotopy perturbation method for MHD flows of UCM fluids above porous stretching sheets. *Comp Math Appl* 59:3328–3337
28. Sajid M, Iqbal Z, Hayat T, Obaidat S (2011) series solution for rotating flow of an upper convected maxwell fluid over a stretching sheet. *Commun Theor Phys* 56:740–744
29. Hayat T, Abbas Z (2007) Channel flow of a Maxwell fluid with chemical reaction. *Z Angew Math Phys (ZAMP)* 59(1):124–144
30. Raftari B, Vajravelu K (2012) Homotopy analysis method for MHD viscoelastic fluid flow and heat transfer in a channel

- with a stretching wall. *Commun Nonlinear Sci Numer Simul* 17(11):4149–4162
31. Bég OA, Makinde OD (2011) Viscoelastic flow and species transfer in a Darcian high-permeability channel. *J Petrol Sci Eng* 76:93–99
 32. Malvandi A, Hedayati F, Ganji DD (2014) Slip effects on unsteady stagnation pointflow of a nanofluid over a stretching sheet. *Powder Technol* 253:377–384
 33. Vajravelu K, Prasad KV, Sujatha A (2012) MHD flow and mass transfer of chemically reactive upper convected Maxwell fluid past porous surface. *Appl Math Mech* 33(7):899–910 (English Edition)
 34. Hatami M, Nouri R, Ganji DD (2013) Forced convection analysis for MHD Al₂O₃–water nanofluid flow over a horizontal plate. *J Mol Liq* 187:294–301
 35. Aziz A (2006) Heat conduction with maple. In: Edwards RT (ed) Philadelphia (PA)
 36. Aziz A (2009) A similarity solution for laminar thermal boundary layer over a flat plate with a convective surface boundary condition. *Commun Nonlinear Sci Numer Simul* 14:1064–1068